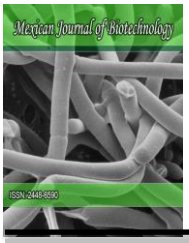

Mexican Journal of Biotechnology 2019, 4(4):1-14

Journal homepage:www.mexjbiotechnol.com
ISSN:2448-6590

ORIGINAL RESEARCH

Biosynthesis of iron nanoparticles (FeNPs) by *Alternaria alternata* MVSS-AH-5

Biosíntesis de nanopartículas de hierro (FeNPs) por *Alternaria alternata* MVSS-AH-5

Diana G. Alamilla-Martínez[1], Norma G. Rojas-Avelizapa[1], Iván Domínguez-López[1], Héctor Pool[2], Marlenne Gómez-Ramírez[1]*

[1]Departamento de Biotecnología, Centro de Investigación en Ciencia Aplicada y Tecnología Avanzada del Instituto Politécnico Nacional, Querétaro, Mexico.
[2]División de Investigación y Posgrado, Facultad de Ingeniería, Universidad Autónoma de Querétaro, Querétaro, Mexico.

*Corresponding author
E-mail address: mgomezr@ipn.mx (M. Gómez-Ramírez)

Article history:
Received: 30 December 2018 / Received in revised form: 26 June 2019 / Accepted: 2 July 2019 / Published online: 1 October 2019.
https://doi.org/10.29267/mxjb.2019.4.4.1

ABSTRACT

The ability of four extracellular filtrates (FE), obtained from *A. alternata* biomass grown in four different culture media; malt dextrose broth (MDB), potato dextrose broth (PDB), sucrose (S) and Czapek (C), were evaluated to biosynthesize iron nanoparticles (FeNPs), at the end of the assay a brown color was revealed in all the samples. To evidence biosynthesis of nanoparticles, absorption spectra were made from 200 to 600 nm for all the samples and, analyzed by transmission electronic microscopy (TEM). The morphology and size of the synthesized FeNPs were studied using the SPIP 6.2.0 software. From the four extracellular filtrates assays, the nanoparticles biosynthesis was possible only in the EF-PDB and EF-C, showing their presence in the UV-vis spectrum when forming an absorption band at 226 and 225 respectively, and plateau around at 270 nm to EF-PDB, and 290 nm to EF-C. The synthesized nanoparticles presented spherical and polydisperse form, those synthesized with EF-PDB showed a size of 20-40 nm, while those synthesized with EF-C had a size of 10-80 nm. Six months after their production, the FeNPs biosynthesized by EF-C were analyzed by microscopy showing an

increase forming 5 µm microparticles, possibly due to magnetic attraction of these materials. To EF-S a peak at 231 nm was detected, but TEM images show formation of iron microcrystals, and iron crystals in EF-MDB which maximum intensity of absorption between 225-303 nm. Culture media used to produce the fungus biomass and get EF have influence in the iron nanoparticles biosynthesis, even in the case of the same microorganism. The FeNPs biosynthesized by *A. alternata* could be used in the removal of contaminants or as microbial agents against bacteria of clinical or agricultural importance.

Keywords: *A. alternate, biosynthesis, extracellular filtrate, FeNPs, nanomaterials*.

RESUMEN

La habilidad de cuatro filtrados extracelulares (FE) obtenidos de la biomasa de *A. alternata* al ser crecida en cuatro medios de cultivo diferentes, nombrados Caldo Malta Dextrosa (CMD), Caldo Papa Dextrosa (CPD), Sacarosa (S) y Czapek (C), fueron evaluados para biosintetizar nanoparticulas de hierro (FeNPs). Para evidenciar la biosíntesis de nanoparticulas se realizó un barrido en el espectro de absorción UV-Vis de 200 a 600 nm a todas las muestras, y analizadas por microscopía electrónica de transmisión (TEM). La forma y tamaño de las FeNPs sintetizadas fue estudiada usando el software SPIP 6.2.0. De los cuatro filtrados extracelulares empleados, la biosíntesis de las nanoparticulas fue posible solo en los FE-CPD y FE-C, evidenciando su presencia en el espectro UV-vis al formar una banda de absorción a los 226 y 225 nm respectivamente, y una meseta alrededor de los 270 nm para el FE-CPD, y 290 nm para el FE-C. Las nanopartículas sintetizadas presentaron forma esférica y polidispersas, las sintetizadas con el FE-CPD presentaron tamaños de 20-40 nm, mientras que las sintetizadas con el FE-C tuvieron tamaños de 10-80 nm. Después de seis meses de producción, las nanopartículas obtenidas con el FE-C se analizaron por microscopía mostrando un aumento de tamaño de hasta 5 µm aproximadamente, posiblemente debido a la atracción magnética de estos materiales. Para el FE-S un pico de 231 nm fue observado pero las imágenes TEM mostraron la formación de microcristales de hierro, y cristales de hierro para el FE-CMD cuya intensidad máxima de absorción estuvo entre los 225 a 303 nm. El medio de cultivo empleado para producir la biomasa del hongo y obtener el FE tiene una influencia en la biosíntesis de nanoparticulas de hierro, aun en el caso del mismo microorganismo. Las FeNPs biosintetizadas por *A. alternata* podrían ser empleadas en la remoción de contaminantes o como agentes microbianos contra bacterias de importancia clínica o agrícola.

Palabras clave: *A. alternata, biosíntesis, FeNPs, filtrado extracellular, nanoparticles*.

1. INTRODUCTION

The metal nanoparticles (NP) like silver nanoparticles (AgNPs), gold nanoparticles (AuNPs), cadmium sulfide nanoparticles (CdSNPs), iron nanoparticles (FeNPs), etc., are nanomaterials with size less than 100 nm. They have interesting applications in different areas of environmental, medicine, energy, agriculture, chemistry, information, communication, heavy industry, and consumer goods, because they have exclusive optical, thermal, and electrochemical properties (Fahmy *et al*., 2018). Biosynthesized NPs can also have enhanced stability and biocompatibility and reduced toxicity, mainly due to coating them with biogenic surfactants or capping agents. The potential range of sizes, shapes and compositions of biosynthesized NPs translates into a broad domain of new nanomaterials applications (Schröfel *et al*., 2014). The FeNPs, has been used since 1990s due to its interesting behavior like presence of high reactive sites, adsorption phenomenon and availability of more surface area (Devatha *et al*., 2018). In the reduction of toxicity of some materials, such is the case of Cr^{+6}, which is converted to Cr^{+3} in wastewater by NA-FE-NPs synthesized by using extract of *Nephrolepis auriculata* (Yi *et al*., 2019). Current applications of iron-based technologies involved remediation process and, are divided into two groups: technologies which use iron as a sorbent, (co-)precipitant or contaminant immobilising agent; and the use of iron as an electron donor to break down or to convert contaminants into a less toxic or mobile form (Bhalerao 2014). As Fento-like catalyst for the decolorization of sodium borohydride (Schröfel et al., 2014), as antibacterial agent of Zero-valent iron nanoparticles (nano-Fe^0) against *Escherichia coli* (Lee *et al.,* 2008), and as antifungal agent against filamentous fungi *Alternaria mali*, *Botryosphaeria dothidea,* and *Diplodia seriata* (Ahmad *et al*., 2017). The Fe_3O_4 NPs (magnetite) have particularly produced great interest in the field of magnetic materials with promising applications for magnetic resonance imaging (MRI), optical, catalysis, environmental remediation, tissue engineering and targeted drug delivery (Patra *et al*., 2017). Biosynthesis of nanoparticles provide some advantages against chemical synthesis, among them it offers an ecofriendly and low-cost production method. The organisms reported as FeNPs producers are principally plants like *Datura inoxia, Calotropis procera, Euphorbia milii, Tinospora cordifolia, Cymbopogon citratus,* and *Tridax procumbens*; the filamentous fungus *Aspergillus oryzae* and bacterium *Acinetobacter spp.* (Fahmy *et al*., 2018). The production of Fe_3O_4 has been reported by magnetotactic bacteria as *Geobacter sulfurreducens, Thermoanaerobacter sp., Thermoanaerobacter ethanolicus* and*, Magnetospirillum magnetotacticum,* has been used to Cr(VI) and Tc(VII) remediation, to enhanced magnetic properties of biosynthesize composite and, cobalt doping of magnetosomes (Schröfel *et al*., 2014). When a fungal biosynthesis of nanoparticles is obtained by extracellular pathway, processes of lysis and purification of the particles is not required. The objective of this research was to evaluate the ability of biosynthesis of four extracellular filtrates of the fungus *Alternaria alternata* MVSS-AH-5 to produce FeNPs from a metallic salt. The FeNPs were biosynthesized only in two extracellular filtrates, thus evidencing that the nutritional conditions affect the expression and excretion of the biomolecules responsible for the synthesis process even with the same organism.

2. MATERIALS AND METHODS

2.1 Microorganism

The filamentous fungus *Alternaria alternata* coded as MVSS-AH-5 was isolated previously from the mine “La Valenciana” from Guanajuato State, in Mexico (Rojas-Avelizapa *et al*., 2017).

2.2 Biomass production and obtaining of extracellular filtrates.

The filamentous fungus was cultivated on potato dextrose agar (PDA) plates and was incubated at 30°C until sporulation. The mycelia were collected and broken using glass beads. The conidia suspension of fungus was determined in a Neubauer chamber. To obtain biomass, four liquid media were assays. Malt dextrose broth (MDB) with composition as follows (g/L): 6.0, Malt extract; 1.8 Maltose; 6.0 Dextrose; 1.2 Yeats extract (Sandoval-Cardenas, 2012). Potato dextrose both (PDB) (Gajbhiye *et al*., 2009). Sucrose medium (S) was composed of (g/L): 100, sucrose; 1.5, $NaNO_3$; 0.5, KH_2PO_4; 0.025, $MgSO_4.7H_2O$; 0.025, KCl; 1.6, yeast extract (Aung & Ting 2005) and, Czapek medium (C) was composed of (g/L): 1,0, K_2HPO_4; 3.0, $NaNO_3$; 0.5, $MgSO_4 \cdot 7H_2O$; 0.5, KCl; 0.01,$FeSO_4 \cdot 7H_2O$; 30.0, sucrose (Deng *et al*., 2013). Four Erlenmeyer flasks of 1000 mL, containing 250 mL of culture medium were, inoculated with fungus conidia to get $3x10^5$ conidia/mL and incubated at 30°C, 150 rpm during 5 days for biomass production. The biomass obtained, was separated by vacuum filtration through sterile fine-pore filter paper, and washed three times with sterile distilled water. Finally, the excess of water was removed through vacuum filtration (Sandoval-Cárdenas *et al*., 2017). The extracellular filtrates were obtained after incubating 5 g of thrice washed biomass with 50 mL of sterile distilled water during 72 h at 30°C and 150 rpm and recovering filtrate trough two filtrations, the first with filter paper and the second using vacuum filtration with a 0.22 µm membrane (Alamilla-Martínez *et al*., 2018). These filtrates biomass free were name extracellular filtrates (EF) and coded according media origin as EF-(MDB), EF-(PDB), EF-S, and EF-C, respectively.

2.3 FeNPs synthesis

Three experimental sets of flasks were prepared for each EF plus $FeSO_4$ salt to reach a final concentration of 1 mM. Negative controls were prepared adding each extracellular filtrate but not $FeSO_4$. The experimental flasks were incubated during 3 days at 45°C and 150 rpm, at the end of incubation period samples were monitored for color change and partially characterized by means of their UV-visible spectra (Sandoval-Cardenas, 2012; Abdelghany *et al*., 2018).

2.4 UV–visible absorption

The FeNPs biosynthesized, were monitored for color change and partially characterized by their UV-vis spectra from 200 to 600 nm. The change in color

from pale orange to brown/black and the increased absorbance at 200-500 nm is indicative of FeNPs formation (Mohamed *et al*., 2015; Devatha *et al*., 2016).

2.5 TEM characterization.

The morphology and size of FeNPs biosynthesized were determined using TEM, all samples were ultrasonically dispersed for eight pulses of 20 seconds and one drop was deposited onto a Cu-collodion-graphite grid and allowed to be air dried. The grid was then scanned employing a JEM10-10 an 80-kV transmission microscope located in the ENCB (Escuela Nacional de Ciencias Biológicas) of IPN. All micrographs were analyzed by using the software SPIP 6.0.2. Nine fields were analyzed per sample and about 150 particles were analyzed (Alamilla-Martínez *et al*., 2018).

3. RESULTS

3.1 FeNPs biosynthesis

The synthesis of iron nanoparticles was initially shows by the color change of the reaction mixture as first indicator of FeNPs synthesis (Patra et al., 2017). The four extracellular filtrates used in this study at the end of incubation period a brown color was revealed in all samples, but confirmation of FeNPs productions was carry out by UV-visible spectrophotometer and analysis TEM. Fig. 1 and 2 show two absorption spectra (A and B) obtained after the FeNPs biosynthesis assay, the four graphs show negative controls (NC) (iron salt and extracellular filtrate separately) and extracellular filtrate plus $FeSO_4$ in triplicate. The spectra obtained from the four extracellular filtrates are show in Fig. 1 and Fig. 2. It was observed that, the number of bands and the intensity of absorption in the region comprising the 200 to 400 nm was broad compared with the intensity of the negative controls, these bands could be indicative of the formation of FeNPs (Mohamed *et al*., 2015; Devatha *et al*., 2016). Surface plasmon resonance (SPR) absorption transition is the most characteristic part of nanoparticles (Patra *et al*., 2017). The maximum intensities of the absorption of EF-MDB were 4.7 a.u. (absorbance units) between 225 to 303 nm (Fig. 1A). In the EF-S a peak of 4.1 a.u. at 231 nm, followed by a plateau around the 265 nm, was detected (Fig. 1B). In the EF-PDB a peak of 3 a.u. was observed at 226 nm followed by a plateau of 2.2 a.u. around 270 nm (Fig. 2A). For EF-C was observed a peak of 2.5 a.u. at 225 nm followed by a plateau of 2 a.u. around the 290 nm (Fig. 2B).

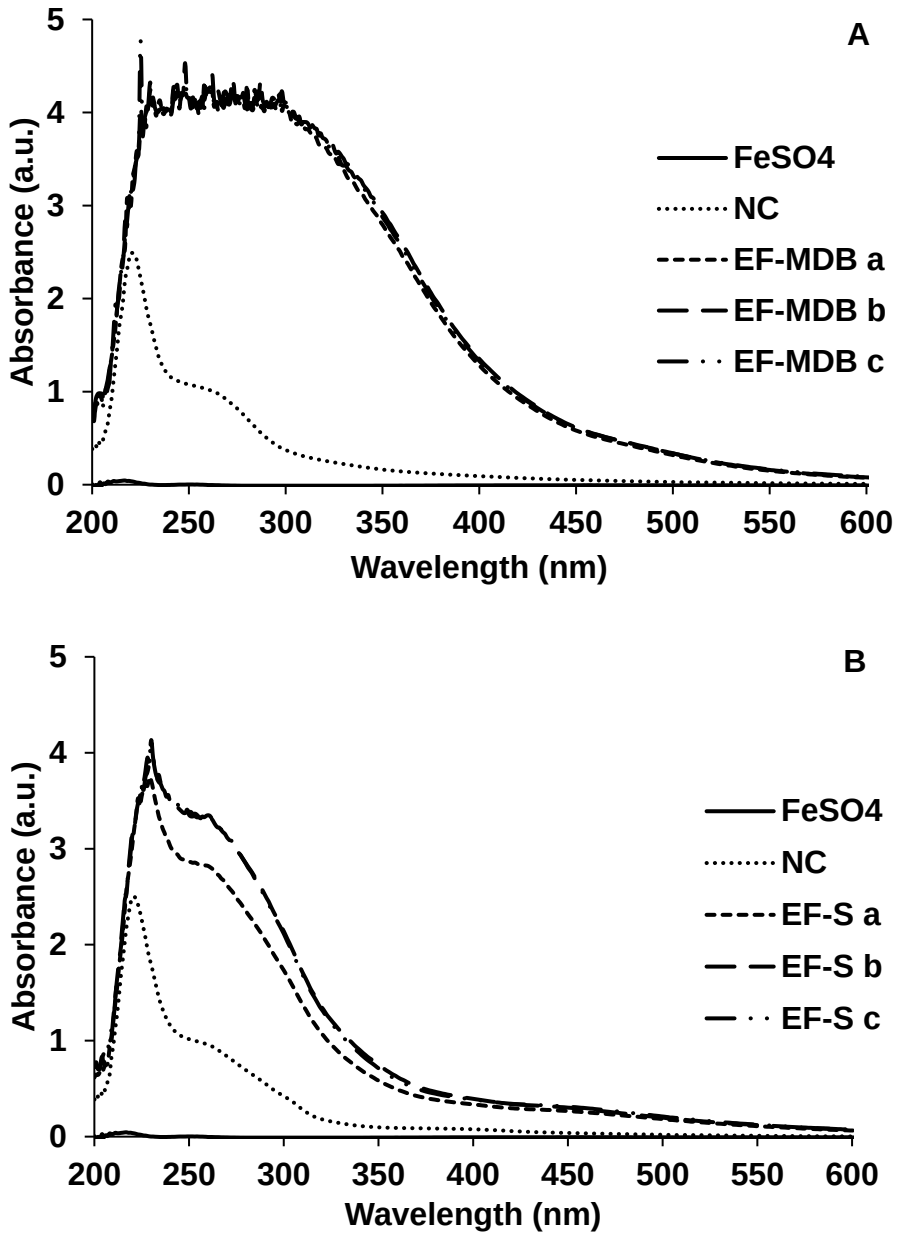

Fig. 1. UV-Vis absorption spectrum of (A) EF-MDB and (B) EF-S with $FeSO_4$ at 1 mM and the negative control (NC), incubated at 45°C during 72 h and 180 rpm in darkness.

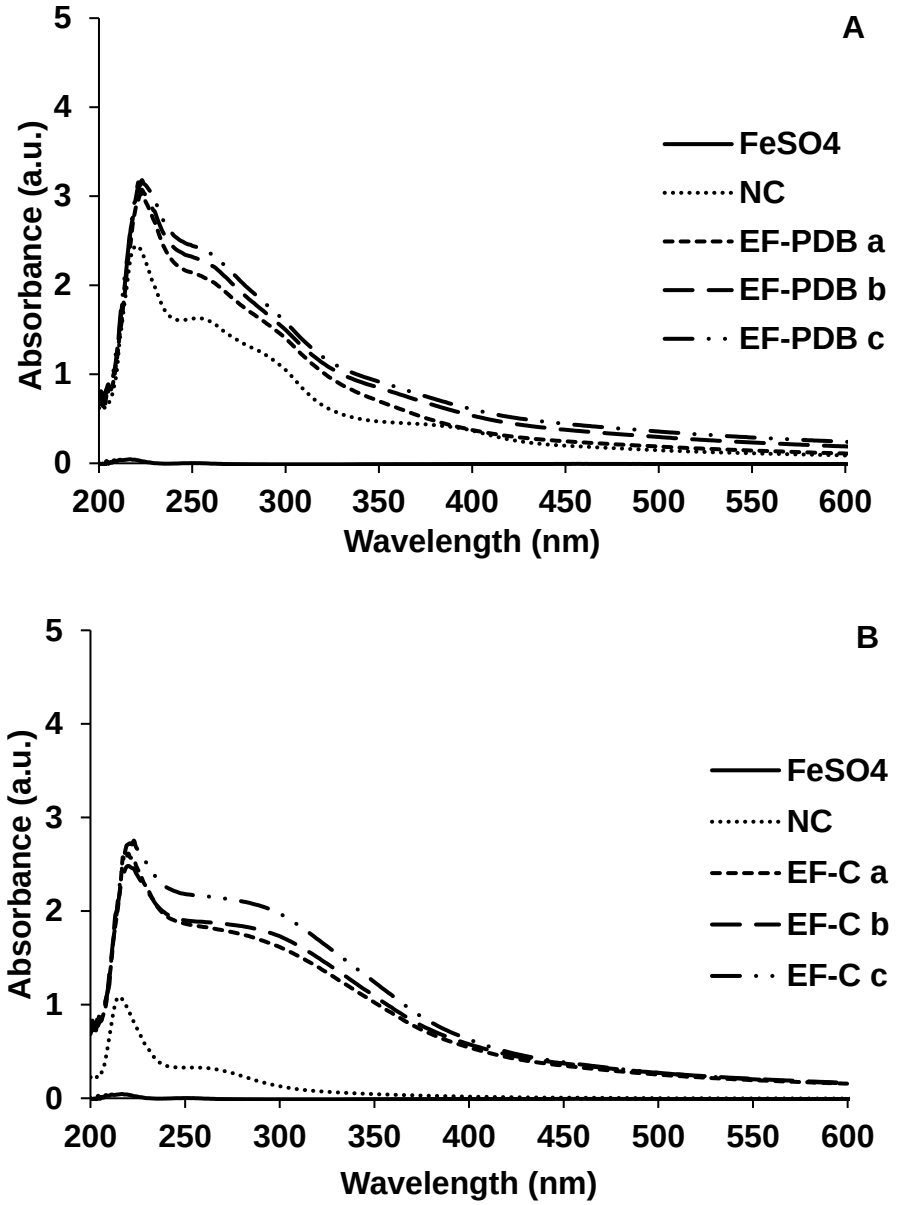

Fig. 2. UV-Vis absorption spectrum of (A) EF-PDB and (B) EF-C with FeSO4 at 1 mM and the negative control (NC), incubated at 45°C during 72 h and 180 rpm in darkness.

3.2 Characterization of FeNPs

All samples obtained by the four EF were analysis by TEM microscopy to demonstrate the presence of FeNPs. Fig. 3A shows nanoparticles of FeNPs synthesized in the filtrate EF-PDB, with semi-oval form whereas in EF-C (Fig. 3B) the FeNPs nanoparticles show morphology spheroid. Fig. 3C shows the formation of agglomerated microcrystals in the filtrates EF-MDB, and larger crystals of 300-500 nm approximately in EF-S (Fig. 3D). After six months of synthesis of FeNPs by EF-C, formation of microparticles of 5 µm was shown (Fig. 3E), probably due to the

highly magnetic nature of the FeNPs, it is known that when nanoparticles has being covered with some organic layer this agglomeration decreases (Lai *et al*., 2018), as could occur in this case because of the biological origin.

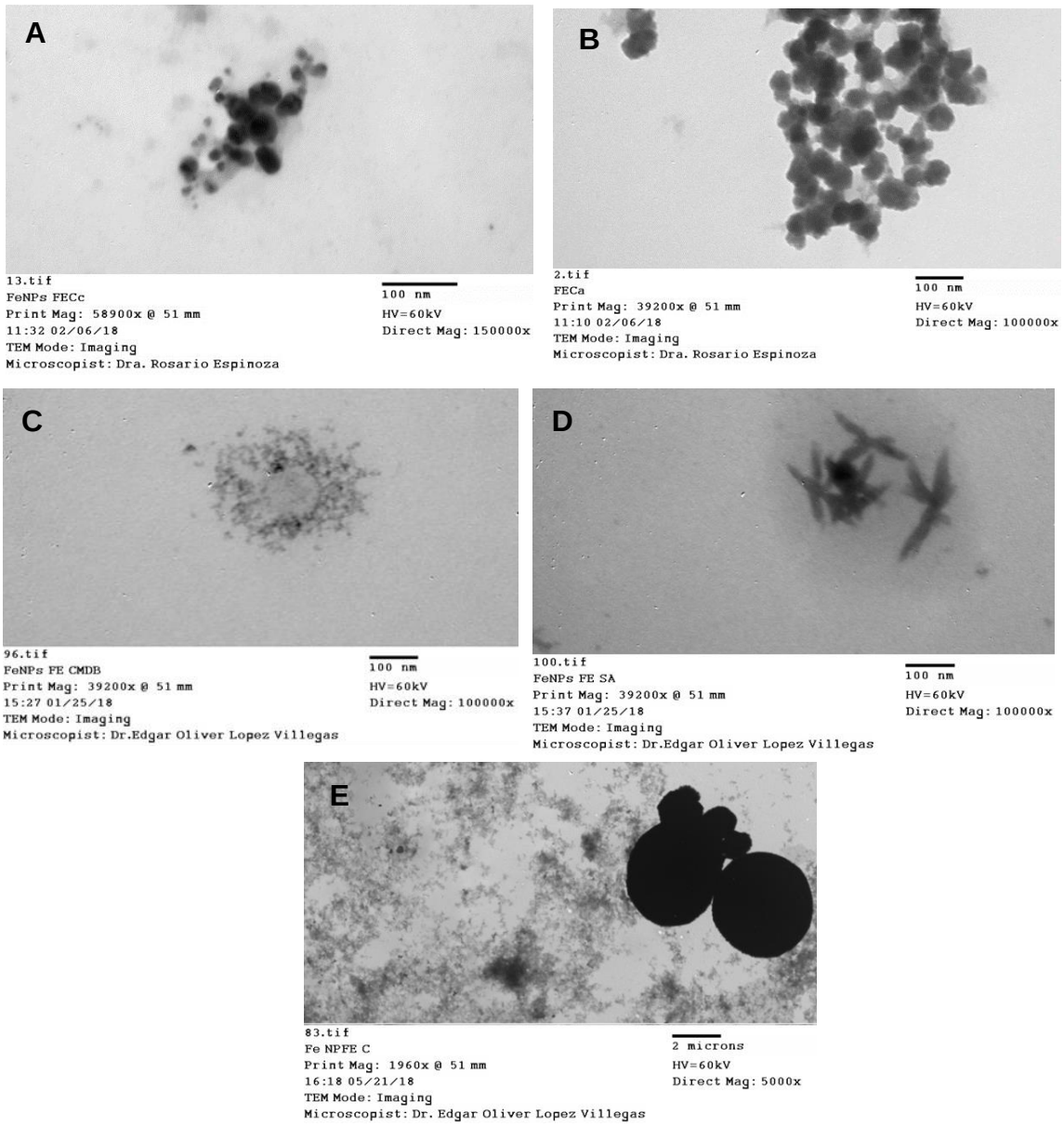

Fig. 3. Micrographs TEM of FeNPs synthetized by fungus *Alternaria alternata* MVSS-AH-5 from EF-PDB and EF-C plus FeSO4 concentration at 1 Mm (A and B), iron microcrystals from EF-MDB (C), and crystal from EF-S (D). Iron microparticles from EF-C after six months at 4ºC (E).

Size of FeNPs synthetized from extracellular filtrates from EF-PDB and EF-C was determined by analysis TEM, and then using the software SPIP 2.0.6, in both cases showed FeNPs polydisperse with size of 20 to 40 nm (33% of 20-30 nm and 39% of 30-40 nm) to EF-PDB, and 10 to 80 nm of diameter to EF-C (Fig. 4). The

low sizes dispersion of the FeNPs biosynthesized from the EF-PDB has a relation with the narrow bandwidth, showed in their absorption spectrum (Fig. 2A), in comparison with the high bandwidth showed in the absorption spectrum of EF-C (Fig. 2B) and its polydisperse size of the FeNPs synthesized.

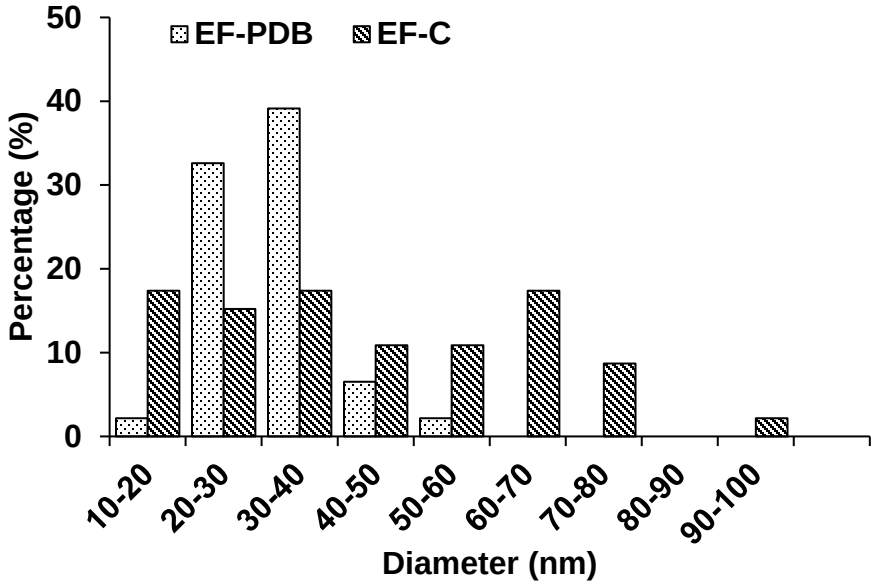

Fig. 4. Size distribution of the FeNPs synthesized for the extracellular filtrate EF-PDB and EF-C at 1 mM of $FeSO_4$, incubated at 45 °C, 180 rpm in darkness during 72 h.

4. DISCUSSION

The synthesis of metallic nanoparticles by fungi is given by the capacity of the molecules excreted toward the extracellular medium to reduce metals, and subsequently stabilize the agglomerations of atoms that are formed when they are in a no-load state, both processes, are made mainly by enzymes and other proteins respectively. Enzymes as hydrogenases, nitrate reductases, naphthoquinones, and, anthraquinones, has been reported as electron shuttle in metal reductions and production of nanoparticles (Durán *et al*., 2005). However, other molecules can also be involved in nanoparticle synthesis for instance, reducing sugars, siderophores, quinone, phenols or molecules with antioxidant activity (Korbekandi *et al*., 2013; Emam *et al*., 2015; Fahmy *et al*., 2018). For the extracellular fungal synthesis of nanoparticles, previously fungal biomass is get in stress by putting it in carbon starvation, in this condition the release of biomolecules its promoted toward the aqueous medium, where nanoparticles biosynthesis is carry out. The type and amount of excreted molecules can be influenced by the nature of the culture media where the fungal mycelium was produced, since the activation of the metabolic pathway required for the utilization of the nutrients present in the culture media depends on this (Alamilla-Martínez *et al*., 2018). During AgNPs biosynthesis by two extracellular filtrate from *Penicillium*

purpurogenum CATMC-AH-1, in EF-Sucrose smallest sizes, and diameter dispersion of AgNPs was obtained, comparing to EF-Czapek. The spherical shape was similar in both filtrates, demonstrated how the culture media where biomass is obtaining to get the extracellular filtrates have an influence on the percentage and size distribution of the biosynthesized AgNPs (Alamilla-Martinez *et al.,* 2018). During synthesis of iron nanoparticles the reduction of Fe^{2+} or Fe $^{3+}$ ions to Fe^{0} is confirmed by visible color change to brown/black depending of nanoparticles concentration in the reaction mixture. Color change indicated the formation of FeNPs physically (Mohamed *et al*., 2015; Devatha *et al*., 2016; Ahmad *et al*., 2017; Asghar *et al*., 2018; Fahmy *et al*., 2018). For the four extracellular filtrates used in this study a brown color was revealed in all samples at the end of the assay, but confirmation of FeNPs was carry out by UV-visible spectrophotometer and analysis TEM. The surface plasmon resonance (SPR) absorption transition is the most characteristic part of nanoparticles, different wavelength emission bands has been identified during biological synthesis of FeNPs (Ahmad *et al*., 2017). In the case of EF-MDB a maximum intensities of the absorption were between 225 to 303 nm (Fig. 1A). A peak at 231 followed by a plateau around the 265 nm in EF-S was detected (Fig. 1B), but TEM images show formation of iron microcrystals, and crystal respectively (Fig. 3C and 3D). As has been observed by Lee *et al* (2008) where nano-Fe^{0} produced and upon exposure to oxygen, nano-Fe^{0} was rapidly oxidized to produce iron precipitates (fibers) on the surface, and a broad UV/visible absorption band centered at around 390 nm evolved as the oxidation of nano-Fe^{0} was observed. On the other hand, in both Filtrates EF-PDB and EF-C, a peak at 226 and 225 nm was detected respectively, a plateau was witnessed around the 270 nm and 290 nm for the EF-PDB and EE-S respectively (Fig. 2A and 2B)., it´s mentioned that Iron oxide nanoparticles shows peak at 222 nm (Mohamed *et al*., 2015). During fungal production of FeNPs by biomass of *A. alternata* two peaks at 238 and 265 nm were detected (Mohamed *et al*., 2015). The peak obtained for FeNPs could varies in the range of 300-500 nm (Devatha *et al*., 2016). A strong peak at 272 nm was detected during bio-fabrication of iron nanoparticles by using *Azadirachta indica* leaf (Ahmad *et al*., 2017), 325 and 296 nm (Devatha *et al*., 2018), 285 and 324 nm; 216 and 265 nm (Fahmy *et al*., 2018), 266 and 274 nm (Asghar *et al*., 2018) all of them using different plant extracts. Magnetic iron oxide (Fe_3O_4) nanoparticles was biosynthesized using aqueous extract of food processing waste, peaks at 330 and 365 nm from MH-FeNPs, and 325 and 365 nm from CCP-FeNPs were detected, absorption band at 355 nm indicated the formation of nano-sized Fe_3O_4 NPs (Patra *et al.,* 2017). Changes in emission wavelength have been describes as a consequence of interaction of NP with immediate surroundings as has been detected in CdS NP (Sandoval-Cárdenas *et al*., 2017). Nevertheless, there are also some molecules that absorb at this wavelength and can interfere, such is the case of aromatic amino acids that absorb at 280 nm (Vigneshwaran *et al*., 2007). Fig. 4 shows the size distribution of both iron nanoparticles biosynthesized, where the characteristics of the FeNPs obtained were of semi-oval and spheroid morphology, polydisperse in both cases, with size in the range of 20-40 nm to EF-PDB, and 10 to 80 nm for EF-C, respectively. In addition, the spectrum band of EF-PDB was narrower than that of EF-C, indicating that possibly the size dispersion of the nanoparticles

biosynthesized in the EF- PDB was low comparing with EF-C. Mohemed *et al* (2015) reported that FePNs biosynthesized by biomass of *A. alternata* had a cubic shape, with average particle diameter of 9 ± 3 nm, the culture medium and production conditions was different to those used in this research. Another sizes and shape of FeNPs has been reported as 20-80 nm (Ahmad *et al*., 2017), amorphous and spherical of 40 to 70 nm (Yi *et al*., 2019), spherical of 5–10 nm (Murgueitio *et al*., 2018), spherical of 96-110 nm (Devatha *et al*., 2018), spherical of 50 to 60 nm (Fahmy *et al*., 2018), spherical of 42-60 nm (Asghar *et al*., 2018). To MH-FeNPs and CCP-FeNPs, sizes of 84.81 and 48.91 nm was detected respectively. Elemental composition by EDX spectroscopy confirmed that Fe_3O_4 NPs were composed of 51.40% Fe, 27.05% Na, 16.10% O and 5.45% Cl for the MH-FeNPs, and of 62.01% Fe, 34.82% Na and 3.17% Cl for the CCP-FeNPs (Patra *et al*., 2017). Characteristics as size and shape of iron nanoparticles obtained by biological synthesis are given by the conditions of production, as well as the extracts plants, EF or biomass used, however amorphous, spherical and cubic shapes, and sizes from 9 to 110 nm has been reported mainly (Mohamed et al., 2015; Ahmad *et al*., 2017; Patra *et al*., 2017; Devatha *et al*., 2018; Fahmy *et al*., 2018; Murgueitio *et al*., 2018; Asghar *et al*., 2018; Yi *et al*., 2019). During bio-fabrication of iron nanoparticles from extracellular filtrate, the molecules involved for the synthesis and stabilization, expressed and excreted depending of the nutritional conditions of growth media where fungal biomass is produced (Singh *et al*., 2013). Previously, Rojas-avelizapa *et al* (2017) reported the ability of *A. alternata* MVSS-AH-5 to produce organics acids, during its growth in sucrose and Czapek media, under this conditions siderophores was produced in media containing sucrose but not in the Czapek media. Siderophores are low molecular weight molecules, and have the ability to bind a variety of metals in addition to iron, the role of siderophores is primarily to scavenge Fe, but they also form complexes with other essential elements (i.e. Mo, Mn, Co, and Ni) in the environment, and make them available for microbial cells (Bellenger *et al*., 2008). For the four extracellular filtrates used to biosynthesis of FeNPs, siderophores presence was detected in the EF-MDB and EF-S while, in EF-PDB and EF-C the amount was minimal (data not show), so the high presence of siderophores in EF-MDB and EF-S, could not allow the nucleation of iron, avoiding the formation of nanoparticles, and catching to form the microcrystals, and crystals that were observed previously (Fig. 3C and 3D). Few report are focus in the employ of fungal biomass, or extracellular filtrate obtained from fungi, however, it`s important to know the factors (nutrition, environmental, etc.) and/or the presence of molecules that can affect or advantage the synthesis of FeNPs when microorganism are used. Iron nanoparticles possess numerous high-tech applications in chemical, electrical, optical, and magnetic fields. The Fe_3O_4 NPs (magnetite) have particularly produced great interest in the field of magnetic materials with promising applications for magnetic resonance imaging (MRI), optical, catalysis, environmental remediation, tissue engineering and targeted drug delivery (Patra *et al*., 2017). These essential applications of FeNPs are essentially associated with their small size, high magnetism, low toxicity and microwave absorption properties (Ahmad *et al*., 2017). In recent years, widespread attention has been directed toward the green synthesis of iron-based nanoparticles (i.e., Fe0, Fe_3O_4, Fe/Ni or Fe/Cu bimetallic

nanoparticles) mainly using plant (Yi *et al*., 2019). There is the importance in the research for new fungi with the ability to biosynthesized FeNPs.

ACKNOWLEDGMENTS

This research received financial support by Project SIP 20171531 and SIP 20181077 of the National Polytechnic Institute.

CONFLICT OF INTEREST

The authors have no conflict of interest to declare.

REFERENCES

Abdelghany T.M., Al-Rajhi A.M.H., Abboud M.A.A., Alawlaqi M.M., Magdah A.G., Helmy E.A.M. & Mabrouk A.S. 2018. Recent advances in green synthesis of silver nanoparticles and their applications: about future directions. A review. BioNanoScience. 8: 5-16.

Ahmad H., Rajagopal K., Shah A.H., Bhat A.H. & Venugpopal K. 2017. Study of bio-fabrication of Iron nanoparticles and their fungicidal property against phytopathogens of apple orchards. IET Nanobiotechnology. 11(3): 230–235.

Alamilla-Martínez D.G., Rojas-Avelizapa N.G., Domínguez-López I. & Gómez-Ramírez M. 2018. Effect of culture media and silver nitrate concentration on nanoparticle biosynthesis by a filamentous fungus. Mexican Journal of Biotechnology. 3(3): 1–14.

Asghar M.S., Zahirb E., Shahid S.M., Khand M.N., Asghare M.A., Iqbalf J. & Walkerf G. 2018. Iron, copper and silver nanoparticles: Green synthesis using green and black tea leaves extracts and evaluation of antibacterial, antifungal and aflatoxin B1 adsorption activity. LWT - Food Science and Technology. 90: 98-107.

Aung K.M.M. & Ting Y.P. 2005. Bioleaching of spent fluid catalytic cracking catalyst using *Aspergillus niger*. Journal of Biotechnology. 116:159–170.

Bellenger J.P., Wichard T., Kustka A.B. & Kraepiel A.M.L. 2008. Uptake of molybdenum and vanadium by a nitrogen-fixing soil bacterium using siderophores. Natural Geosciences. 1: 243–246.

Bhalerao T.S. 2014. A review: applications of iron nanomaterials in bioremediation and in detection of pesticide contamination. International Journal of Nanoparticles. 7(1): 73-80

Deng X., Chai L., Yang Z., Tang C., Wang Y. & Shi Y. 2013. Bioleaching mechanism of heavy metals in the mixture of contaminated soil and slag by using indigenous *Penicillium chrysogenum* strain F1. Journal of Hazardous Materials.

248–249: 107–114.

Devatha C.P., Thalla A.K. & Katte S.Y. 2016. Green synthesis of iron nanoparticles using different leaf extracts for treatment of domestic waste water. Journal of Cleaner Production. 139: 1425-1435.

Devatha C.P., Jagadeesh K. & Patil M. 2018. Effect of green synthesized iron nanoparticles by *Azardirachta Indica* in different proportions on antibacterial activity. Environmental Nanotechnology, Monitoring & Management. 9: 85-94.

Durán N., Marcato P.D., Alves O.L., De Souza G.IH. & Esposito E. 2005. Mechanistic aspects of biosynthesis of silver nanoparticles by several *Fusarium oxysporum* strains. Journal of Nanobiotechnology. 3: 8.

Emam H.E., El-Rafie M.H., Ahmed H.B. & Zahran M.K. 2015. Room temperature synthesis of metallic nanosilver using acacia to impart durable biocidal effect on cotton fabrics. Fibers and Polymers. 16(8): 1676–1687.

Fahmy H.M., Mohamed F.M., Marzouq M.H., Mustafa A.B.E-D., Alsoudi A.M., Ali O. A., Mahmed M.A. & Mahmound F.A. 2018. Review of green methods of iron nanoparticles synthesis and applications. BioNanoScience. 8(2): 491–503.

Gajbhiye M., Kesharwani J., Ingle A., Gade A. & Rai M. 2009. Fungus-mediated synthesis of silver nanoparticles and their activity against pathogenic fungi in combination with fluconazole. Nanomedicine: Nanotechnology, Biology, and Medicine. 5(4): 382–386.

Korbekandi H., Ashari Z., Iravani S. & Abbasi S. 2013. Optimization of biological synthesis of silver nanoparticles using *Fusarium oxysporum.* Iranian Journal of Pharmaceutical Research. 12(3): 289–98.

Lai C.W., Low F.W., Tai M.F. & Hamid S.B.A. 2018. Iron oxide nanoparticles decorated oleic acid for high colloidal stability. Advances in Polymer Technology. 37(6), 1712–1721.

Lee C., Kim J.Y., Lee W.I., Nelson K.L., Yoon J. & Sedlak D.L. 2008. Bactericidal Effect of Zero-Valent Iron Nanoparticles on *Escherichia coli*. Environmental Science & Technology. 9(1): 19–22.

Mohamed Y.M., Azzam A.M., Amin B.H. & Safwat N.A. 2015. Mycosynthesis of iron nanoparticles by *Alternaria alternata* and its antibacterial activity. African Journal of Biotechnology. 14(14): 1234–1241.

Murgueitio E., Cumbal L., Abril M., Izquierdo A., Debut A. & Tinoco O. 2018. Green synthesis of iron nanoparticles: Application on the removal of petroleum oil from contaminated water and soils. Journal of Nanotechnology. 2018: 8p.

Patra J.K & Baek K-H. 2017. Green biosynthesis of magnetic iron oxide (Fe_3O_4) nanoparticles using the aqueous extracts of food processing wastes under photo-catalyzed condition and investigation of their antimicrobial and antioxidant activity. Journal of Photochemistry & Photobiology, B: Biology. 173: 291-300.

Rojas-Avelizapa N.G., Otamendi-Valdez J. & Gómez-Ramírez M. 2017. Metal leaching from a spent catalyst by *Alternaria alternata*. Mexican Journal of Biotechnology. 2(2): 221–231.

Sandoval-Cárdenas D.I. 2012. Uso de hongos microscópicos aislados de muestras ambientales para la producción de nanopartículas de plata. Instituto Politécnico Nacional. Queréaro, México.

Sandoval-Cárdenas I., Gómez-Ramírez M. & Rojas-Avelizapa N.G. 2017. Use of a sulfur waste for biosynthesis of cadmium sulfide quantum dots with *Fusarium oxysporum f. sp. lycopersici*. Materials Science in Semiconductor Processing. 63: 33-39.

Schröfel A., Kratošová G., Šafařík I., Šafaříková M., Raška I. & Shor L.M. 2014. Applications of biosynthesized metallic nanoparticles - A review. Acta Biomaterialia. 10(10): 4023-4042.

Singh R., Wagh P., Wadhwani S., Gaidhani S., Kumbhar A., Bellare J. & Chopade B.A. 2013. Synthesis, optimization, and characterization of silver nanoparticles from *Acinetobacter calcoaceticus* and their enhanced antibacterial activity when combined with antibiotics. International Journal of Nanomedicine. 8: 4277-4290.

Vigneshwaran N., Ashtaputre N.M., Varadarajan P.V, Nachane R.P., Paralikar K. M. & Balasubramanya R.H. 2007. Biological synthesis of silver nanoparticles using the fungus *Aspergillus flavus*. 61(6): 1413-1418.

Yi Y., Tu G., Tsang P.E., Xiao S. & Fang Z. 2019. Green synthesis of iron-based nanoparticles from extracts of *Nephrolepis auriculata* and applications for Cr(VI) removal. Materials Letters. 234: 388–391.